(Preprint) AAS 11-207

SENSITIVITY OF MAGNETOSPHERIC MULTI-SCALE (MMS) MISSION NAVIGATION ACCURACY TO MAJOR ERROR SOURCES

Corwin Olson,* Anne Long,† and J. Russell Carpenter‡

The Magnetospheric Multiscale (MMS) mission consists of four satellites flying in formation in highly elliptical orbits about the Earth, with a primary objective of studying magnetic reconnection. The baseline navigation concept is independent estimation of each spacecraft state using GPS pseudorange measurements referenced to an Ultra Stable Oscillator (USO) with accelerometer measurements included during maneuvers. MMS state estimation is performed onboard each spacecraft using the Goddard Enhanced Onboard Navigation System (GEONS), which is embedded in the Navigator GPS receiver. This paper describes the sensitivity of MMS navigation performance to two major error sources: USO clock errors and thrust acceleration knowledge errors.

INTRODUCTION

The Magnetospheric Multiscale (MMS) mission consists of four satellites with identical instrument suites flying in formation in highly elliptical orbits about the Earth. The primary objective of the mission is to study the phenomenon known as magnetic reconnection, which is a process that converts magnetic energy into heat and kinetic energy of charged particles. After launching into highly elliptical orbits and perigee raising maneuvers to place the spacecraft in orbits with a 1.2 Earth Radii (Re) perigee and 12 Re apogee, the mission begins with the commissioning phase in which initial testing of all spacecraft systems will occur. Phase 1a begins when the orbit has evolved such that the apogee is on the day side of the Earth. In Phase 1 the formation separations will be adjusted from 160km to 10km in an effort to study reconnection on the dayside boundary between the solar wind and the Earth's magnetosphere known as the "bow shock" region. The following period when the apogee is once again on the night side of the Earth is Phase 1x, after which Phase 1b starts when the apogee has returned to the dayside. During Phase 2a, a series of apogee raising maneuvers are executed to incrementally increase the orbital apogee of each spacecraft from 12 Re to 25 Re. Phase 2b will begin when the apogee raising for all four spacecraft is complete. During Phase 2b the formation separations will vary from 400km to 30km, with the optimum separation chosen by mission scientists after the full range of different formation sizes has been executed. During Phase 2b the mission will study the

* Aerospace Engineer, a.i. solutions, Inc., 10001 Derekwood Lane, Suite 215, Lanham, Maryland USA 20706.
† Chief Systems Engineer, a.i. solutions, Inc., 10001 Derekwood Lane, Suite 215, Lanham, Maryland USA 20706.
‡ Aerospace Engineer, Code 595, NASA Goddard Space Flight Center, Greenbelt, Maryland USA 20771.

night-side reconnection events that occur in the Earth's magneto-tail. After Phase 2b, the mission will end and the spacecraft will be de-commissioned. Reference 1 contains a more detailed description of the mission concept.[1]

Figure 1 shows the high-level navigation concept for MMS along with the configuration of each spacecraft's navigation and attitude control elements. Each spacecraft's state is independently estimated using Global Positioning System (GPS) pseudorange measurements referenced to an Ultra Stable Oscillator (USO). MMS state estimation is performed onboard each spacecraft using the Goddard Enhanced Onboard Navigation System (GEONS), which is embedded in the Navigator GPS receiver. The Navigator GPS receiver employs a new weak signal tracking technology that significantly improves reception of GPS signals when the spacecraft is above 10 Re.[2] Thrust acceleration measurements from an accelerometer within the Attitude Control System are included during maneuvers. The estimated state consists of the position, velocity, clock bias, clock bias rate, and clock bias acceleration. The estimated states are periodically downlinked and used in the MMS Flight Dynamics Operations Area (FDOA) to generate definitive and predictive products to support mission and science operations.

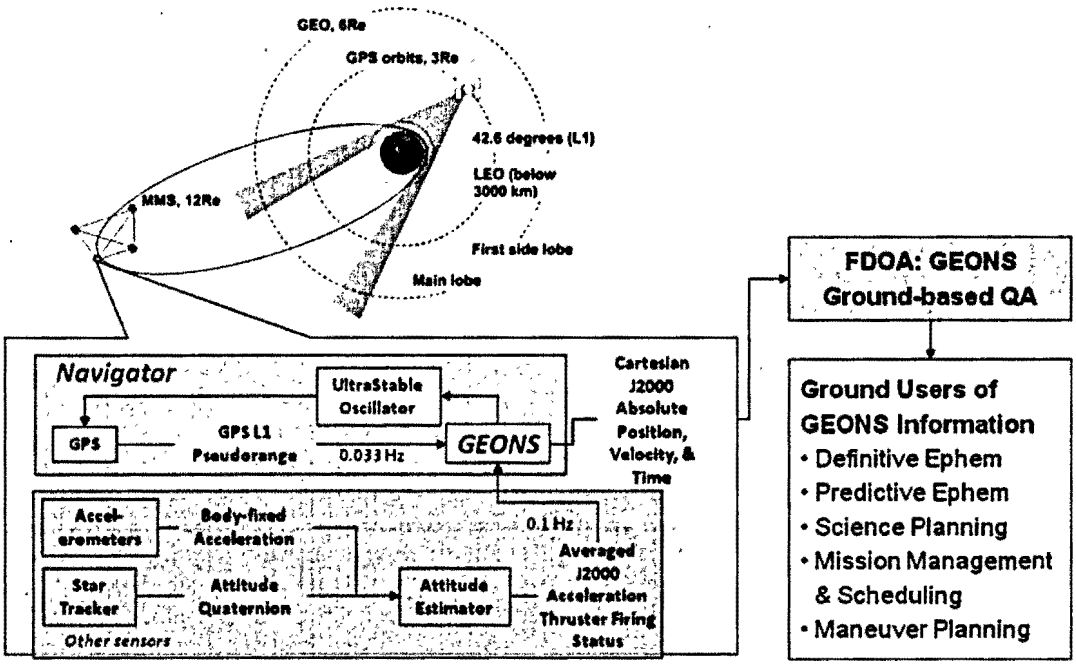

Figure 1. Navigation Concept and Onboard Configuration.

Navigation knowledge error, or the difference between the estimated state and the truth state, can be attributed to a number of different sources. The primary contributors include the truncation of the onboard gravity model to 8x8 due to onboard processing limitations, solar radiation pressure (SRP) modeling errors, GPS pseudorange measurement noise, GPS ephemeris errors, receiver clock errors, and thrust acceleration knowledge errors. This paper examines the sensitivity of MMS navigation performance to USO clock errors and thrust acceleration knowledge errors. An understanding of this sensitivity is needed to ensure that all mission requirements are met, especially if the USO clock or accelerometers do not perform as expected during the mission.

The MMS mission imposes several challenging navigation requirements due to the fact that the majority of the orbital period occurs above the GPS constellation where GPS signal acquisition is sparse. Critical requirements include the following[3]:

- A maximum USO clock bias error of 325 microseconds is needed to meet the science requirement for a maximum relative clock bias error of 1 millisecond between spacecraft.
- A maximum definitive Brouwer-Lyddane mean semi-major axis (SMA) error of 100m above 3 Re is needed to meet formation maintenance maneuver planning requirements.
- A maximum relative definitive position error of 1% of the separation or 100m, whichever is larger, is needed to meet science requirements.
- A maximum relative predicted position error growth of 200 m/day is needed to meet collision avoidance requirements.

The USO clock error model parameters that were varied in this analysis include the clock process noise parameters and the amplitudes of the aging affect and umbra-induced temperature variations. The thrust acceleration knowledge error model parameters that were varied in this analysis include the direction bias, magnitude bias, magnitude drift due to random walk, magnitude scale factor, and temperature variation. These values are varied in an effort to determine the sensitivity of absolute and relative position and velocity navigation error and clock bias errors to these error sources.

This analysis uses as a baseline a segment of the mission Phase 2b. Phase 2b is the most challenging phase of the mission for navigation because there are significantly fewer GPS measurements acquired for a much greater percentage of the orbit, and the receiver must propagate through over 2.1 days of the 2.8 day orbit without GPS measurements during apogee due to onboard power constraints. During the simulation time span, the nominal formation scale size (approximate distance between spacecraft during the science region of interest) is 30 kilometers. The simulation includes a pair of formation maintenance maneuvers, which are designed to maintain the quality of the spacecraft formation. The first of these two maneuvers occurs immediately after exiting the science Region-of-Interest (ROI), which is defined as the region above 15 Re for Phase 2b. The second maneuver is immediately before re-entering the science ROI, after traveling through perigee. A pair of Phase 2b formation maintenance maneuvers for a 400km formation size scenario along with the final two maneuvers of the apogee raising sequence in Phase 2a are also examined to determine the sensitivity of navigation error to acceleration errors during a longer maneuver. Due to page length limitations, the Phase 2b 400km separation and Phase 2a results are only briefly summarized below.

SIMULATION METHODOLOGY

Figure 2 outlines the simulation methodology that was employed for this analysis. The Mission Design (MD) code is used to generate the truth trajectory and the truth finite maneuvers, and the truth trajectory is fed into the Measurement Data Simualtion (DatSim) program to generate GPS pseudorange (PR) measurements. The accelerations from the truth finite maneuvers are modified to include knowledge error. The measurements and accelerations with knowledge error are ingested into GEONS, which generates estimates of the state and covariance values for the state. These states and covariance values are used along with the truth ephemeris to compute errors and verify requirements.

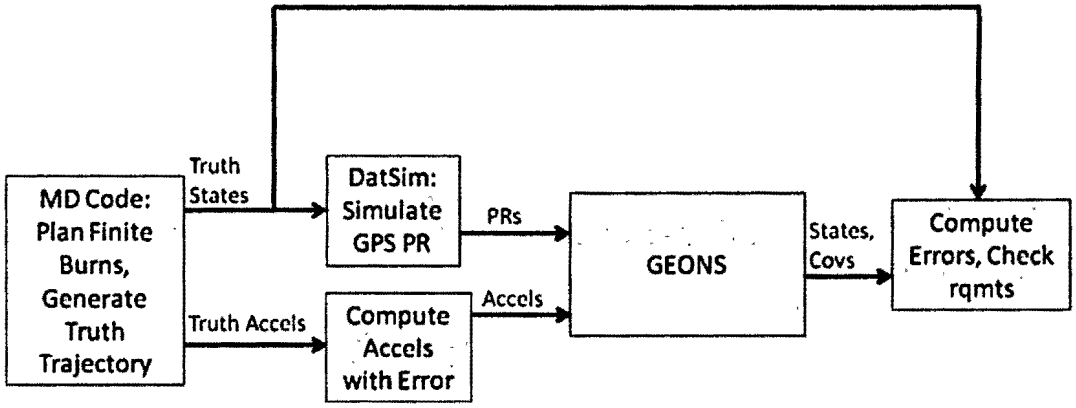

Figure 2. Simulation Methodology.

TRUTH TRAJECTORY GENERATION PROCEDURE

Figure 3 illustrates the procedure used to generate the truth trajectory and maneuver accelerations. The End-to-End (ETE) code referenced in the procedure is a code set designed to simulate all phases of the MMS mission from commissioning to the end of Phase 2b as one continuous simulation in order to verify all mission design and Conjunction Assessment (CA) requirements.

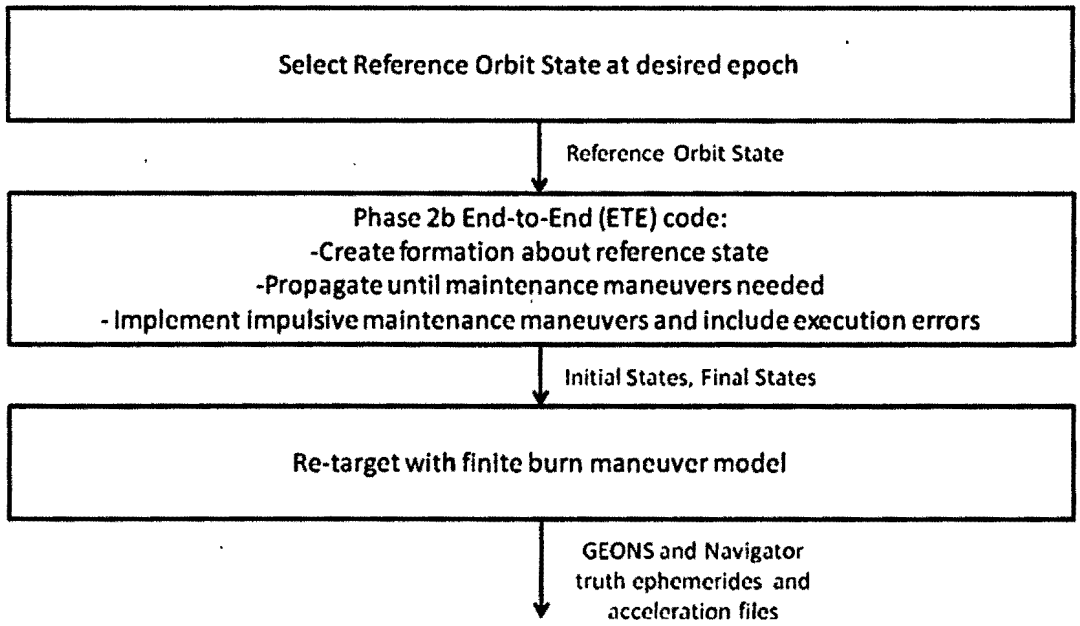

Figure 3. Truth Trajectory Generation Procedure.

TRAJECTORY MODELS, MEASUREMENT MODEL, FILTER SETTINGS

Table 1 lists the primary models and associated values used to propagate the truth and filtered trajectory of each MMS spacecraft. The truth trajectory was generated using the FreeFlyer mission analysis software application. The GEONS filter models are consistent with the models being used to support the MMS mission, which are tailored to execute within the limited resources of the flight processor within the Navigator receiver.

Table 1. Trajectory Propagation Models.

Simulation Parameter	FreeFlyer Truth	GEONS Filter
Nonspherical Earth Gravity Model	21x21 Joint Gravity Model-2	8x8 Joint Gravity Model-2
Point Mass Gravity	Sun, Moon using DE 405 ephemeris	Sun, Moon using analytical fit to DE 406 ephemeris
Atmospheric Drag	Analytical constant temperature hydrostatic model, C_D of 2.2, Drag area of 7.1 m^2	Analytical fit to Harris Priester model, C_D of 2.2, Drag area of 7.1 m^2
Solar Radiation Pressure	Spherical model, C_R of 1.8, SRP area of 2.026712 m^2	Spherical model, C_R of 1.8, SRP area of 2.02 m^2
Integrator	8(9) Variable Step Runge-Kutta	4^{th} Order Fixed Step Runge-Kutta
Integration Stepsize	10 seconds	30 seconds
Maneuver Model	Finite burns	Accelerometer measurements averaged over 10 seconds, including acceleration knowledge errors

Table 2 lists the simulation parameter values used for measurement simulation. These values were selected to match the measured performance of the Navigator GPS receiver for specific ranges of the signal-to-noise-ratio (C/N0) value.

Table 2. Measurement Acquisition and Error Models.

Simulation Parameter	Nominal Values
Measurement Type	GPS Pseudoranges (PR)
Navigator Receiving Antenna	Composite torroidal model for spinning spacecraft with peak gain normal to the spin axis
GPS PR Measurement Rate	1 Measurement set every 30 seconds for each formation member, with measurements from a maximum of 12 visible GPS SVs when below 15Re, no measurements above 15Re in Phase 2b
GPS Acquisition Threshold (Based on Navigator Performance)	C/N0 $\geq$ 40 dB-Hz: 95% probability of acquisition, minimum acquisition delay of 600 sec C/N0 = 28 to 40 dB-Hz: 75% probability of acquisition, minimum acquisition delay of 600 sec C/N0 < 28 dB-Hz: 0% probability of acquisition
GPS Antenna Model	GPS IIA with Transmitting Antenna Effective Isotropic Radiated Power (SVEIRP) = 13.4 dB-Hz
GPS Constellation	21+3 GPS Space Vehicles
GPS Space Vehicle (SV) Selection	Min to max Transmitter ID values
1σ GPS PR Noise (Based on Navigator Specifications)	4 meters for C/N0 $\geq$ 40 dB-Hz (strong signal) 10 meters for C/N0 < 40 dB-Hz (weak signal)
GPS Ephemeris and Clock Errors	Sinusoidal ephemeris model with 2 meter amplitudes for each component
Ionospheric Delay Model	GPS Ionospheric Model based on GPS broadcast coefficients

Table 3 lists the parameters incorporated in the GEONS filter, which is a UD factorized extended Kalman filter.[4]

Table 3. GEONS Filter Settings.

Parameter	Nominal Values
Estimation State	Position, velocity, clock bias, clock bias rate, clock bias acceleration
Initial position and velocity state errors	300 m and 15 mm/sec per axis (1σ)
Initial Clock bias, drift, and acceleration errors	150 km (500 μs) (1σ), 46 mm/s, 2.3 μm/s^2
GPS PR standard deviation	40 m
Minimum Height of Ray Path Altitude	1000 km (eliminates measurements with largest ionospheric delays)

SENSITIVITY TO USO CLOCK ERRORS

The following analysis was conducted to determine the sensitivity of onboard clock bias, drift, and acceleration estimation for the MMS mission to various clock stability parameters. These parameters include clock process noise parameters and the amplitudes of the aging effect and Umbra Temperature Events. The effect of aging refers to the change in the clock bias acceleration as time passes after the USO is turned on. Umbra Temperature Events are sinusoidal variations in the clock bias acceleration that have a period equal to the orbital period and are applied for every orbit to represent the worst case where for every orbit the spacecraft enters the umbra of the Earth. An understanding of this sensitivity is important due to the 325 microsecond requirement on clock bias knowledge. This requirement is most challenging during periods without GPS measurements when the clock bias must be propagated.

These parameters are set by the user in the DatSim program, which generates measurements for the simulation.[5] Process Noise Variance Rates (PNVRs) for the clock parameters were modified as necessary in GEONS to ensure that the filter used to estimate the state was properly tuned. The USO clock error model is described in detail below.

USO Truth Clock Model

The truth clock model incorporates the following parameters: initial clock bias, initial clock drift, initial clock acceleration, frequency white noise, frequency random walk, frequency random run, aging model amplitude and time constant, and the amplitude, start, and stop times for periodic variations due to umbra-related temperature changes.

The clock bias acceleration due to the aging effect is described in the equation

$$\ddot{b}_r^{aging}(t_i) = \frac{b_1}{[t_i - t_0] + b_2} \tag{1}$$

where the coefficients b_1 and b_2 are determined by fitting to empirical data to characterize the magnitude and effective rate of decay, t_i is the current time and t_0 is the initial time.

Solar and lunar umbras produce temperature variations during the orbital period in which the umbra event occurs. The effect of frequency variations that occur due to temperature variations before, during, and after umbras are modeled by including a clock bias acceleration term for each umbra interval. This term is modeled as a sinusoidal variation, with amplitude equal to b_3 and period equal to the duration of the event:

$$\ddot{b}_r^{event}(t_i) = \begin{cases} b_3 \cos\left(\dfrac{2\pi\left(t_i - t_{start}^{event}\right)}{t_{end}^{event} - t_{start}^{event}}\right); \text{if } t_{start}^{event} < t_i \le t_{end}^{event} \\ 0; \text{otherwise} \end{cases} \tag{2}$$

The value of b_3 is related to a change in temperature as described in the equation

$$b_3 = \frac{2\pi}{P}\frac{\Delta f_r(t_i)}{f_r(t_i)} = \frac{2\pi}{P} f_1 \cdot \frac{\Delta^\circ C}{2} \tag{3}$$

where f_1 is the change in the fractional frequency per 1°C change in temperature, and P is the period that is equal to the duration of the event, modeled as one orbital period.

The full truth clock propagation is performed sequentially as follows:

$$\begin{bmatrix} b_r(t_{i+1}) \\ \dot{b}_r(t_{i+1}) \\ \ddot{b}_r(t_{i+1}) \end{bmatrix} = \begin{bmatrix} 1 & \Delta T & \dfrac{\Delta T^2}{2} \\ 0 & 1 & \Delta T \\ 0 & 0 & 1 \end{bmatrix} \begin{bmatrix} b_r(t_i) \\ \dot{b}_r(t_i) \\ \ddot{b}_r(t_i) \end{bmatrix} + \begin{bmatrix} 0 \\ 0 \\ \Delta\ddot{b}_r^{aging}(t_{i+1}) + \Delta\ddot{b}_r^{event}(t_{i+1}) \end{bmatrix} + Q \begin{bmatrix} \varepsilon_1 \\ \varepsilon_2 \\ \varepsilon_3 \end{bmatrix} \tag{4}$$

$$\begin{aligned} \Delta\ddot{b}_r^{aging}(t_{i+1}) &= \ddot{b}_r^{aging}(t_{i+1}) - \ddot{b}_r^{aging}(t_i) \\ \Delta\ddot{b}_r^{event}(t_{i+1}) &= \ddot{b}_r^{event}(t_{i+1}) - \ddot{b}_r^{event}(t_i) \end{aligned} \tag{5}$$

where ΔT is the clock prediction step size in seconds and Q is the clock noise matrix, defined below. The values ε_1, ε_2, and ε_3 are normally distributed deviates with zero mean and unit variance, which can be initialized with the same or different random number seeds.

For the correlated clock error model used in this analysis, the components of the clock noise matrix Q is defined such that QQ^T is equal to the full clock covariance matrix:

$$QQ^T = \begin{bmatrix} q_1\Delta T + q_2\dfrac{\Delta T^3}{3} + q_3\dfrac{\Delta T^5}{20} & q_2\dfrac{\Delta T^2}{2} + q_3\dfrac{\Delta T^4}{8} & q_3\dfrac{\Delta T^3}{6} \\ q_2\dfrac{\Delta T^2}{2} + q_3\dfrac{\Delta T^4}{8} & q_2\Delta T + q_3\dfrac{\Delta T^3}{3} & q_3\dfrac{\Delta T^2}{2} \\ q_3\dfrac{\Delta T^3}{6} & q_3\dfrac{\Delta T^2}{2} & q_3\Delta T \end{bmatrix} \tag{6}$$

where Q is the upper right triangular matrix given by

$$Q = \begin{bmatrix} \sqrt{q_1\Delta T + q_2\dfrac{\Delta T^3}{12} + q_3\dfrac{\Delta T^5}{720}} & \sqrt{q_2\Delta T + q_3\dfrac{\Delta T^3}{12}}\dfrac{\Delta T}{2} & \sqrt{q_3\Delta T}\dfrac{\Delta T^2}{6} \\ 0 & \sqrt{q_2\Delta T + q_3\dfrac{\Delta T^3}{12}} & \sqrt{q_3\Delta T}\dfrac{\Delta T}{2} \\ 0 & 0 & \sqrt{q_3\Delta T} \end{bmatrix} \tag{7}$$

and where q_1, q_2, and q_3 are process noise variance rates associated with frequency white noise, frequency random walk, and frequency random run, respectively. The input simulation parameters h_0 and h_{-2} are white noise and random walk Allan variances that are related to the process noise variance rates q_1 and q_2 as shown in the equations

$$q_1 = \frac{h_0}{2}$$
$$q_2 = 2\pi^2 h_{-2} \tag{8}$$

The baseline scenario for this analysis was the MMS Phase 2b, 30km separation case. Table 4 lists the baseline clock error parameters used in the measurement simulation software for each satellite for Phase 2b. These values are consistent with the expected performance of the USOs being procured for MMS. Table 4 also shows the clock model values used in the GEONS filter for this study.

Table 4. Baseline Clock Error Model Parameters.

Simulation Parameter	Truth Model Value	GEONS Filter Value
Initial Bias	3.6343×10^{-3} s	3.0655×10^{-3} s
Initial Rate	1.54×10^{-10} s/s	0.0 s/s
Initial Acceleration	2.0×10^{-15} s/s^2	0.0 s/s^2
Frequency White Noise q_1	$1.2E10^{-22}$ s^2/s (h_0=2.4×10^{-22})	Not Modeled
Frequency Random Walk q_2	1.58×10^{-26} s^2/s^3 (h_{-2}=8×10^{-28})	
Frequency Random Run q_3	10^{-38} s^2/s^5	
Aging Amplitude b_1, Time Constant b_2	5×10^{-9}, 10 days (from turn-on)	
Periodic Variation Amplitude $b_3 = (2\pi/P)10^{-11}(\Delta C)$ (s/s^2)	3.7 h umbra in Phase 2b: 2.0×10^{-15}	

Variations Performed

The clock parameters were varied in a systematic method to examine the sensitivity of onboard position, velocity, clock bias, clock drift, and clock acceleration estimation performance to the various clock stability parameters. The parameters varied include the noise parameters h_0, h_{-2}, and q_3, as well as the amplitude of the aging affect b_1 and the Umbra Temperature Events b_3. Process Noise Variance Rates (PNVRs) for the clock parameters were modified as necessary in GEONS to ensure proper tuning.

Table 5 below contains the variations of the clock model that were conducted for this analysis. The first run was with the baseline values that were consistent with the expected performance of the USOs being procured for the MMS Navigator receivers. Next each term was increased in magnitude to assess the sensitivity to degraded performance.

Table 5: Baseline and Successive Clock Model Variations

Case	h_0 (s^2/s)	h_{-2} (s^2/s^3)	q_3 (s^2/s^5)	b_1 (s/s)	b_3 (s/s^2)
Baseline MMS clock	2.4E-22	8E-28	1E-38	5E-09	2E-15
h_0 * 100	**2.4E-20**	8E-28	1E-38	5E-09	2E-15
h_{-2} * 100	2.4E-22	**8E-26**	1E-38	5E-09	2E-15
q_3 * 100	2.4E-22	8E-28	**1E-36**	5E-09	2E-15
b_1 * 2	2.4E-22	8E-28	1E-38	**10E-09**	2E-15
b_3 * 2	2.4E-22	8E-28	1E-38	5E-09	**4E-15**
All values increased	**2.4E-20**	**8E-26**	**1E-36**	**5E-09**	**4E-15**

Phase 2b Orbit Radius and GPS Visibility

During Phase 2b, the MMS spacecraft receives far fewer GPS measurements when it is above the GPS constellation than when it is below the GPS constellation and no measurements at all when it is above 15 Re due to onboard power constraints. This lack of measurements results in propagation over long periods of time which can lead to large state errors, especially if maneuvers have occurred. As a result, Phase 2b is the most challenging phase of the mission for navigation of the spacecraft.

Figures 4 and 5 display the MMS satellite radial distance from the Earth and the number of GPS satellites (SVs) visible during the simulated segment of Phase 2b. These figures show the large variation in the number of visible GPS satellites as a function of satellite radial distance. When compared with plots of estimation error results shown in the next section, the relationship between the number of GPS satellites tracked by the receiver and the estimation state error is apparent.

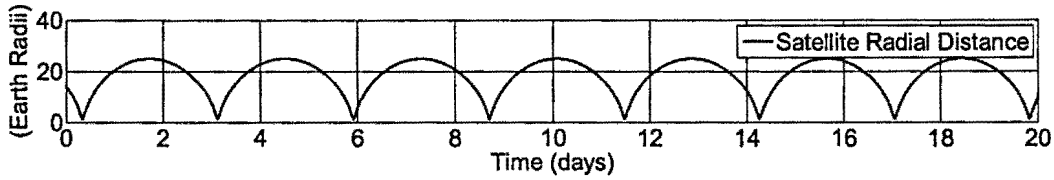

Figure 4. Satellite Orbital Radius in Earth Radii for Phase 2b.

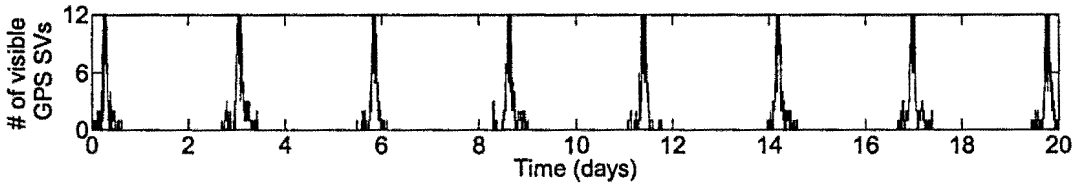

Figure 5. Number of GPS Satellites Visible for Phase 2b.

Clock Model Sensitivity Results

All results below are for spacecraft MMS 1, which is representative of the sensitivity trends seen for the other spacecraft. The first case was run using the baseline clock model as described in Table 5, the results of which were compared to each variation described in Table 5. Figure 6 shows the clock bias, drift, and acceleration error and formal standard deviation estimated by the filter with baseline clock settings as defined in Table 5. Comparing Figure 6 to the GPS visibility plot in Figure 5, the clock state error starts to grow when GPS measurements are no longer available and continues to grow until measurements are once again received, at which point the error drops dramatically to much smaller levels. The periodic variations in the clock acceleration error are due to the presence of umbra variations in the clock truth, but not in the clock estimation model.

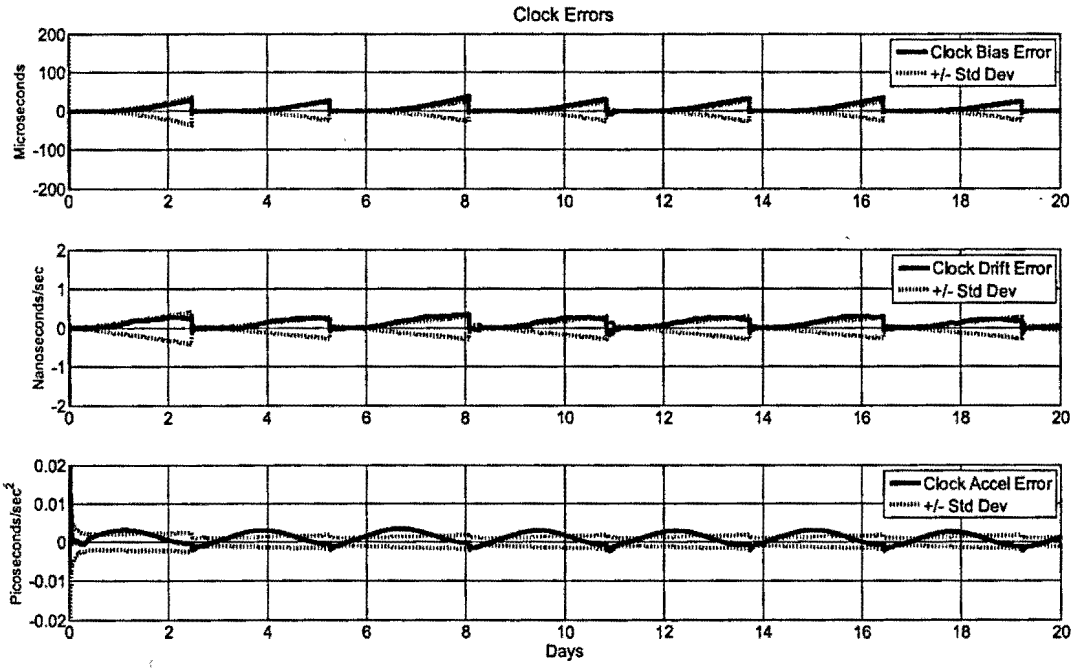

Figure 6. Clock Bias, Drift, Acceleration Error and Covariance with Baseline Clock Settings.

Figures 7 and 8 show the RSS position and velocity errors along with the filter's formal standard deviation for the baseline case defined in Table 5. The points labeled M1 and M2 are the times of the first and second formation maintenance maneuvers. Notice that the error increases significantly immediately after M2 because after knowledge errors are induced by M2 the estimated state must be propagated for about 50 hours through apogee until GPS measurements are once again acquired by the receiver.

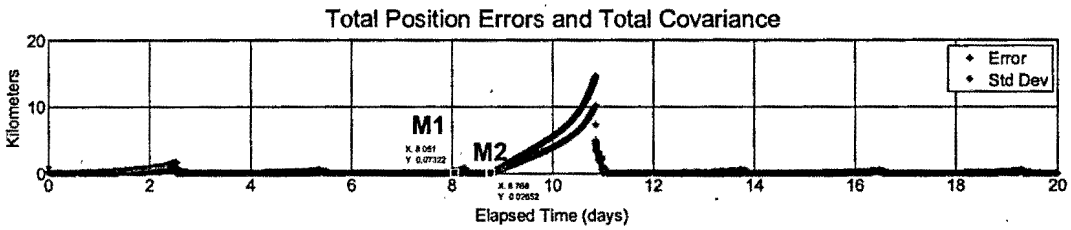

Figure 7. Position Error and Covariance with Baseline Clock Settings.

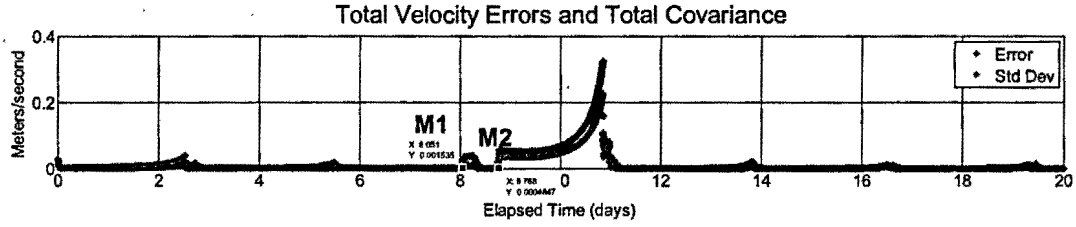

Figure 8. Velocity Error and Covariance with Baseline Clock Settings.

It was determined that, of the initial variations, only the cases that increased h_2 and b_3 produced significant changes in the clock bias, drift, and acceleration error. All cases met the 325

microsecond clock prediction accuracy requirement, but if the h_{-2} parameter is increased by another order of magnitude to $8x10^{-25}$, the requirement is violated. This indicates that the h_{-2} parameter has the smallest allowable variation in order to meet the requirement.

Figure 9 shows the clock bias, drift, and acceleration error and covariance with the Random Walk Allan Variance h_{-2} clock parameter increase as defined as h_{-2} * 100 in Table 5. It is clear that the increase of the h_{-2} parameter introduces significantly more bias, drift, and acceleration.

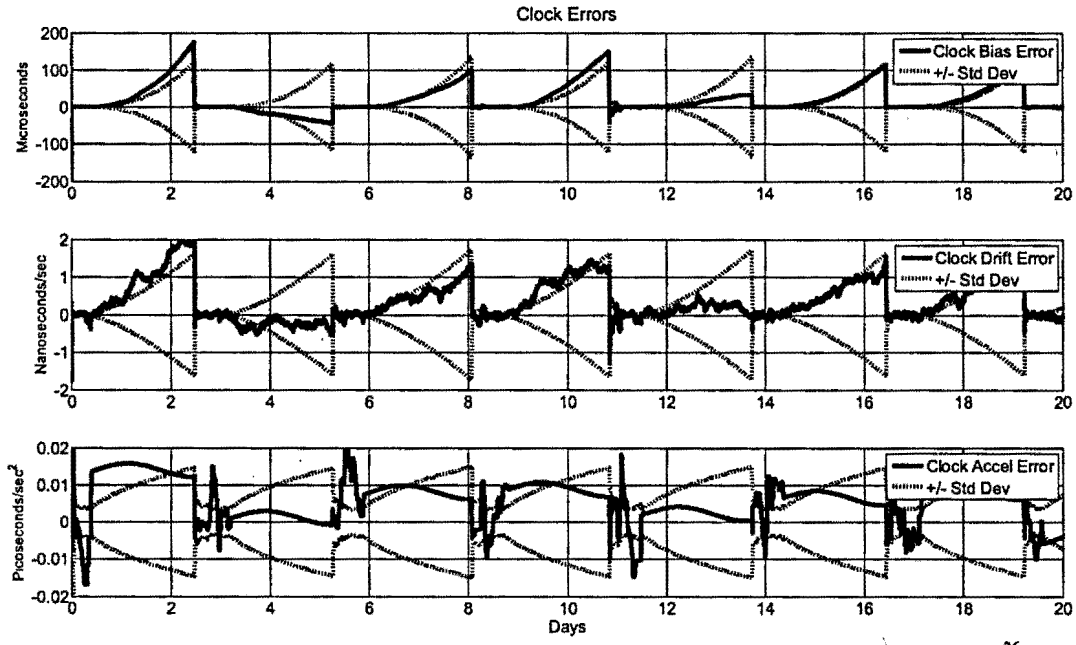

Figure 9. Clock Bias, Drift, Acceleration Error and Covariance with h_{-2} Increased to $8x10^{-26}$.

Figures 10 and 11 show the RSS position and velocity errors along with covariance for the h_{-2} clock parameter increase as defined in Table 5. When the filter is appropriately tuned, this case did not have a significant impact on the position and velocity errors over the propagation period immediately following the second maneuver, as the additional error introduced was absorbed by the clock states.

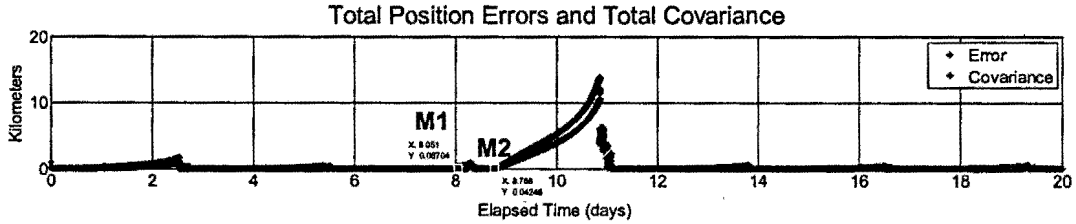

Figure 10. Position Error and Covariance with h_{-2} Increased to $8x10^{-26}$.

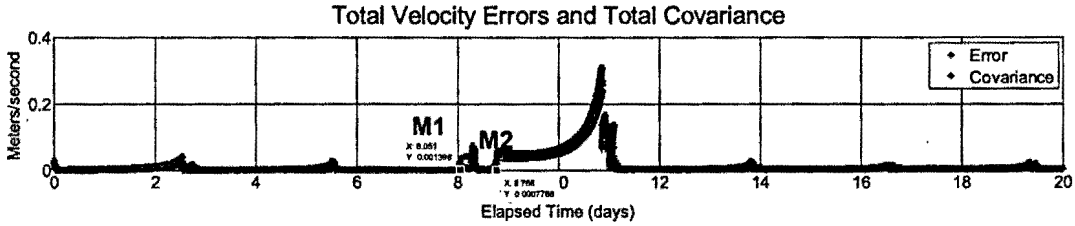

Figure 11. Velocity Error and Covariance with h_2 Increased to $8x10^{-26}$.

Figures 12, 13 and 14 below illustrate the maximum clock bias, RSS position, and RSS velocity errors that result from the nominal baseline case and each variation. For all cases, the maximum position and velocity errors occur after the second maneuver. It is clear that the h_2 increase case, as well as the b_3 increase case, produce significantly larger levels of clock bias error as compared to the baseline. Position and velocity errors are not sensitive to these changes.

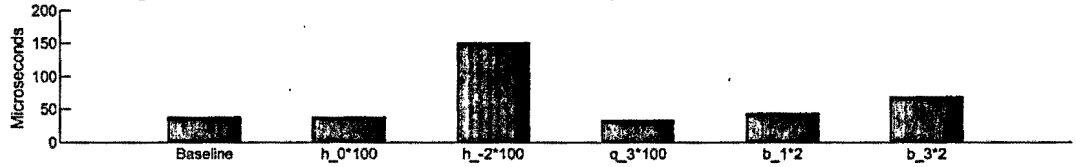

Figure 12. Maximum Clock Bias Error for Each Primary Clock Error Parameter Variation.

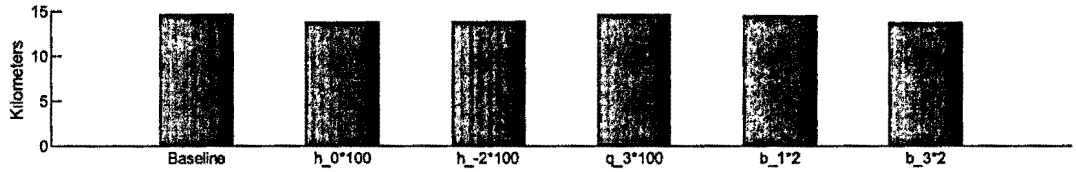

Figure 13. Maximum RSS Position Error for Each Primary Clock Error Parameter Variation.

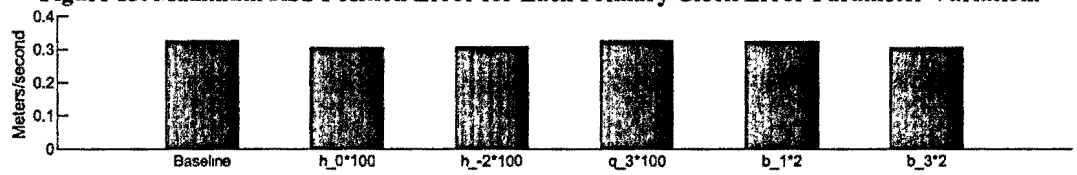

Figure 14. Maximum RSS Velocity Error for Each Primary Clock Error Parameter Variation.

SENSITIVITY TO THRUST ACCELERATION KNOWLEDGE ERRORS

The MMS onboard accelerometers will generate 10-second averaged acceleration measurements that GEONS will process during each maneuver. In order to simulate these measurements, an acceleration knowledge error model was developed for each formation maintenance and apogee raising maneuver that includes errors that are consistent with the expected "worst case" acceleration knowledge errors.

Thrust Acceleration Knowledge Error Model

The Guidance, Navigation and Control (GN&C) subsystem will convert the raw acceleration measurements in the body frame to the mean of J2000 inertial (MJ2000.0) frame using the spacecraft attitude, and then average these values over 10 seconds to the nearest whole 10 second mark. Table 6 below describes the thrust acceleration knowledge error model parameters, which were derived from analysis conducted by the MMS GN&C subsystem team, and which include a 50% modeling uncertainty factor.

Table 6. Thrust Acceleration Knowledge Error Model Parameters.

Parameter	1σ Value
Direction Bias (dir_{mag}) – Formation Maintenance Maneuvers	0.681°
Direction Bias (dir_{mag}) – Apogee Raising Maneuvers	0.447°
Magnitude Bias $(bias_{mag})$	1.5 μg
Magnitude Drift $(drift_{mag})$	22.5 μm/s/s$^{1/2}$
Magnitude Scale Factor $(ScaleFactor)$	0.01625%

The thrust acceleration knowledge error model provides the perturbed acceleration vector expressed in the MJ2000.0 frame averaged over a 10 second interval, $\vec{a}_{with\_error}$, given by

$$\vec{a}_{with\_error} = \vec{u}_{pert\_inertial}\left(\|\vec{a}\|(10\,\text{sec}) + \Delta Verr_{mag}\right)/(10\,\text{sec}) \tag{9}$$

where $\vec{u}_{pert\_inertial}$ is the direction of the perturbed acceleration vector in the MJ2000.0 frame, $\|\vec{a}\|$ is the magnitude of the true acceleration, and $\Delta Verr_{mag}$ is the total delta-v magnitude error, as detailed below.

The total delta-v magnitude error is computed as the sum of the following contributions:

$$\Delta Verr_{mag}(t) = \Delta Verr_{mag\_bias} + \Delta Verr_{mag\_ScaleFactor}(t) + \Delta Verr_{mag\_TempVar}(t) + \Delta Verr_{drift}(t) \tag{10}$$

The delta-v magnitude bias $(\Delta Verr_{mag\_bias})$ which will be applied at every acceleration time throughout the maneuver, is calculated using the equation

$$\Delta Verr_{mag\_bias} = (bias_{mag})(10\,\text{sec})RV_{gauss} \tag{11}$$

where $bias_{mag}$ is 1.5 μg, or 1.5 * 9.81 * 10^{-6} m/s^2, and RV_{gauss} is a random number value generated from a Gaussian distribution of mean equal to 0 and standard deviation equal to 1.

The error due to a scale factor on the delta-V is shown in the equation

$$\Delta Verr_{mag\_ScaleFactor}(t) = ScaleFactor_{VarOn}\|\vec{a}(t)\|(10\,\text{sec})RV_{gauss} \tag{12}$$

where $\vec{a}(t)$ is the true average acceleration corresponding to time t in the acceleration file and the scale factor value to be used at each acceleration time is varied in a sinusoidal fashion:

$$ScaleFactor_{VarOn} = ScaleFactor + (3\times10^{-6})(0.5°C)\sin\left(\tfrac{2\pi}{T}\Delta t\right) \tag{13}$$

where *ScaleFactor* is 0.01625%, T is the period of the temperature sinusoidal variation which is 60 minutes for this analysis, and Δt is the time that has elapsed since the maneuver start time.

The magnitude error due to temperature variations assuming a 3 μg/°C bias sensitivity is

$$\Delta Verr_{mag\_TempVar}(t) = (3\times10^{-6})(9.81\,m/s^2)(0.5°C)\sin\left(\tfrac{2\pi}{T}\Delta t\right) \tag{14}$$

The drift error due to random walk is computed at every acceleration time within the maneuver:

$$\Delta Verr_{drift}(t) = \Delta Verr_{drift}(t_{prev}) + \left(drift_{mag}\right)\sqrt{t - t_{prev}}\,RV_{gauss}(t) \tag{15}$$

where t_{prev} is the previous acceleration time, $\Delta Verr_{drift}(t_{prev})$ is the drift error from the previous acceleration time within the maneuver, and $RV_{gauss}(t)$ is a random number value generated at every acceleration time in the maneuver. For this analysis, $t - t_{prev}$ is 10 seconds.

The delta-v direction bias that is applied at every acceleration time throughout the maneuver is determined using the cone-and-clock method. The angle of the cone, i.e. the angle between the acceleration vector and the error vector as shown in Figure 15, is

$$\theta = cone\ angle = \left|\left(dir_{mag}\right)RV_{gauss}\right| \tag{16}$$

The clock angle, i.e. the point on the circle formed by the cone that will be selected as the direction of the error vector as shown in Figure 15, is given by

$$\phi = clock\ angle = (360°)RV_{uniform} \tag{17}$$

where $RV_{uniform}$ is a random number value generated from a uniform distribution on the open interval 0 to 1.

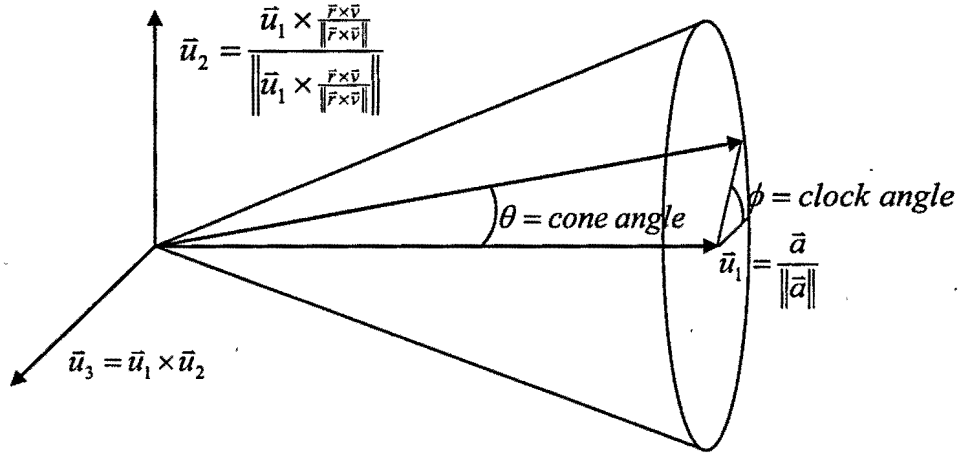

Figure 15. Direction Error Cone.

The reference frame in which the error is computed must be defined in inertial space at every acceleration time within the maneuver. Three unit vectors are defined: 1) $\vec{u}_1$, along the direction of the acceleration in the inertial frame, 2) $\vec{u}_2$, along the cross product between the first unit vector and the orbital angular momentum vector unit vector, and 3) $\vec{u}_3$, along the cross product between the first two unit vectors. Thus the unit vector of the acceleration vector with direction error at a particular time is expressed in the inertial frame as

$$\vec{u}_{err\_inertial} = [\vec{u}_1\ \vec{u}_2\ \vec{u}_3]R_1(\phi)R_2(\theta)\begin{bmatrix}1 & 0 & 0\end{bmatrix}^T \tag{18}$$

where $R_1(\phi)$ is a rotation matrix about the first axis, $R_2(\theta)$ is a rotation matrix about the second axis, and $[\vec{u}_1\ \vec{u}_2\ \vec{u}_3]$ is the rotation matrix that transforms the unit vector from the acceleration frame to the inertial frame.

Variations Performed

The parameters of the acceleration knowledge error model that were varied included Direction Bias for Formation Maintenance (FM), Direction Bias for Apogee Raising (AR), Magnitude Bias, Magnitude Drift due to random walk, Magnitude Scale Factor Error, and Magnitude Error due to Temperature Variations. Starting with the same Phase 2b 30km scenario that was used for the USO off nominal analysis, the thrust acceleration knowledge error model values used for the Baseline were 10% of the 1-σ values listed in Table 6. The 10% percentage was chosen because it produces results similar to the Phase 2b 30km baseline scenario that was used for the USO off nominal analysis. In each variation performed, the individual parameter value was increased by an order of magnitude to the 1-σ value, as described in Table 7. These are the actual values used for each parameter, i.e. they are not sampled randomly. 1-σ values were chosen because the difference in results between the cases were more discernable than when smaller values were chosen for the variations.

Table 7. Baseline and Successive Acceleration Knowledge Error Model Variations.

Case	Direction Bias (FM)	Direction Bias (AR)	Magnitude Bias	Magnitude Drift	Scale Factor	Temperature
Baseline	0.0681°	0.0447°	0.15 μg	2.25 μm/s/s$^{1/2}$	0.001625%	0.3 μg/°C
Direction Bias (FM) increased	**0.681°**	0.0447°	0.15 μg	2.25 μm/s/s$^{1/2}$	0.001625%	0.3 μg/°C
Direction Bias (AR) increased	0.0681°	**0.447°**	0.15 μg	2.25 μm/s/s$^{1/2}$	0.001625%	0.3 μg/°C
Magnitude Bias increased	0.0681°	0.0447°	**1.5 μg**	2.25 μm/s/s$^{1/2}$	0.001625%	0.3 μg/°C
Magnitude Drift increased	0.0681°	0.0447°	0.15 μg	**22.5 μm/s/s$^{1/2}$**	0.001625%	0.3 μg/°C
Scale Factor increased	0.0681°	0.0447°	0.15 μg	2.25 μm/s/s$^{1/2}$	**0.01625%**	0.3 μg/°C
Temperature increased	0.0681°	0.0447°	0.15 μg	2.25 μm/s/s$^{1/2}$	0.001625%	**3 μg/°C**
All values increased	**0.681°**	**0.447°**	**1.5 μg**	**22.5 μm/s/s$^{1/2}$**	**0.01625%**	**3 μg/°C**

Phase 2b 30km Formation Maintenance Maneuver Results

All results below are for spacecraft MMS 1, which is representative of the sensitivity trends seen for the other spacecraft. The clock error, RSS position error, and RSS velocity error for the baseline case are shown in Figures 16 through 18.

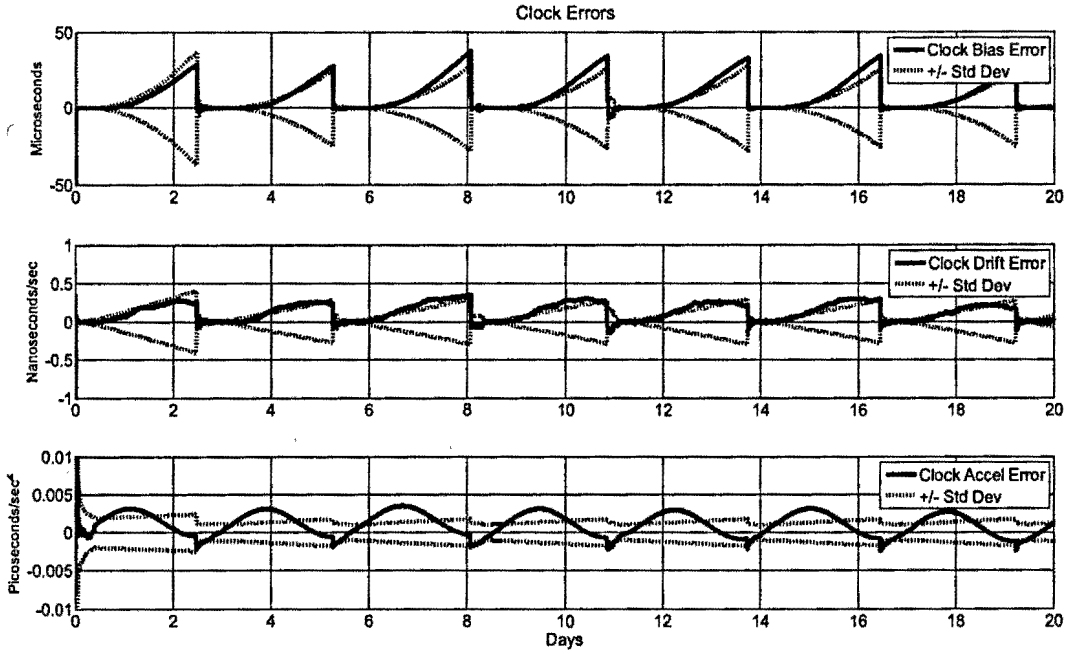

Figure 16. Baseline Clock Bias, Drift, Acceleration Error and Covariance.

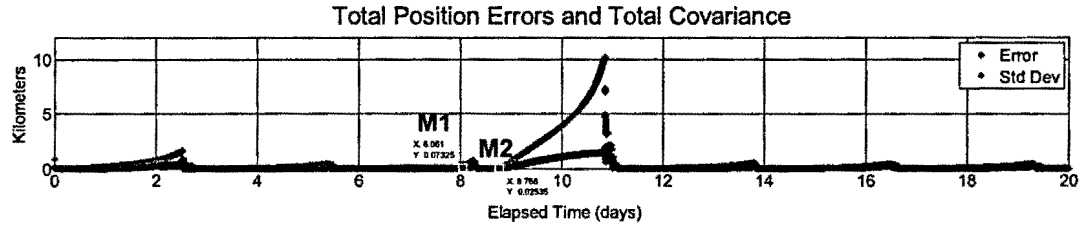

Figure 17. Baseline RSS Position Error and Covariance.

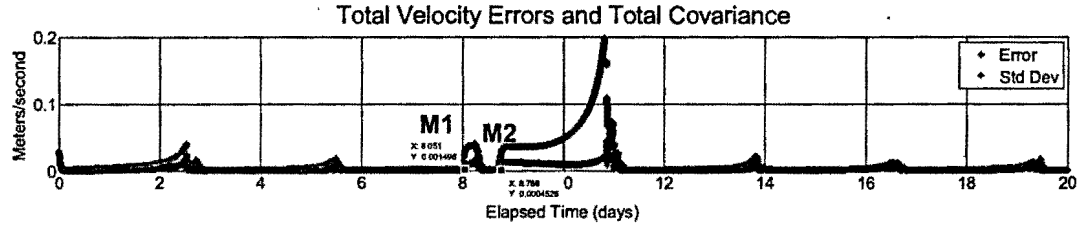

Figure 18. Baseline RSS Velocity Error and Covariance.

Figure 19 shows the maximum RSS position error for all Phase 2b 30km cases described in Table 7, with the same trends seen in maximum RSS velocity error for each case. These values reveal that the position and velocity error are most sensitive to the magnitude drift.

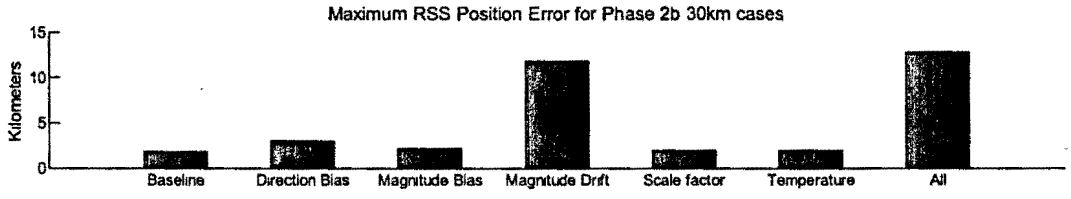

Figure 19. Maximum RSS Position Error for Phase 2b 30km Cases.

The increase of the magnitude drift parameter results in very slightly modified clock error, indicating a minimal sensitivity of the clock error to acceleration knowledge errors. Figures 20 and 21 show the RSS position and velocity errors with the direction bias parameter increase as defined in Table 7. The increase of the magnitude drift parameter had a significant impact on the position and velocity errors over the propagation period immediately following the second maneuver. The position and velocity error was significantly different only in the time between the second maneuver and the following perigee passage, and to a much smaller degree the orbit following this perigee passage.

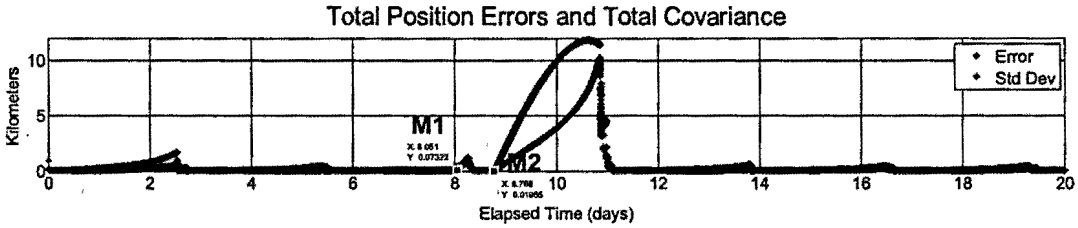

Figure 20. Position Error and Covariance with Magnitude Drift Increased to 1-σ.

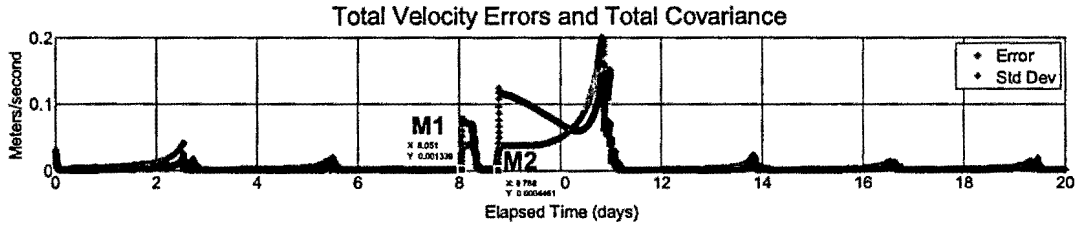

Figure 21. Velocity Error and Covariance with Magnitude Drift Increased to 1-σ.

Phase 2b 400km Formation Maintenance Maneuver Results

Phase 2b 400km was considered in addition to Phase 2b 30km because the maneuvers were significantly larger than those in Phase 2b 30km, which allowed for an investigation of how the size of the maneuver affects the sensitivities. The size of the maneuvers for the Phase 2b 400km scenario were on the order of 6 to 11 meters per second, versus those for the Phase 2b 30km scenario, which were on the order of 1 to 3 meters per second. The same sensitivity patterns were seen for Phase 2b 400km as were seen in Phase 2b 30km, except that the direction bias increase did not produce a significant change in the maximum RSS position or velocity error values.

Phase 2a Apogee Raising Maneuver Results

The thrust acceleration knowledge error for the longer Apogee Raising maneuvers in Phase 2a were also varied using the same method as for Phase 2b 30km described previously, however it was determined that due to the fact that the Apogee Raising maneuvers occur when the spacecraft is receiving GPS measurements, the impact of thrust acceleration knowledge errors is minimal.

CONCLUSION

This study indicated that increases in the clock drift random walk parameter h_{-2} produces the largest increases in the navigation error among the USO clock error model parameters, with a secondary sensitivity to the amplitude of the umbra temperature events b_3. The maximum clock bias error observed in each primary clock error model variation was well below the maximum clock bias error requirement of 325 microseconds, indicating significant margin. For the thrust acceleration knowledge error model parameters, it was determined that for both shorter and longer maneuvers, the total navigation error is primarily sensitive to knowledge magnitude drift due to velocity random walk during the maneuver. However, this sensitivity is only significant when there are long periods of propagation following the maneuver.

REFERENCES

[1] C. Gramling, "Overview of the Magnetospheric MultiScale Formation Flying Mission," *AAS/AIAA Astrodynamics Specialists Conference,* August 2009. Paper AAS 09-328.

[2] J. R. Carpenter, "Magnetospheric Multi-Scale Mission's Orbit Propagation Sensitivity to Navigation Errors," *AAS/AIAA Astrodynamics Specialists Conference,* August 2009. Paper AAS 09-323.

[3] P. T. Scaperoth, A. Long, and J. R. Carpenter, "Magnetospheric MultiScale (MMS) Phase 2b Navigation Performance," *AAS/AIAA Astrodynamics Specialists Conference,* August 2009. Paper AAS 09-324.

[4] a.i. solutions, Inc., FDSS-14-0002, *Goddard Enhanced Onboard Navigation System (GEONS) Mathematical Specifications, Release 2.14*, A. Long et al., prepared by a.i. solutions, Inc., November 2010.

[5] a.i. solutions, Inc., FDSS-14-0005, *User's Guide and Mathematical Specifications for the Measurement Data Simulation Program, Release 2.14*, A. Long et al., prepared by a.i. solutions, Inc., November 2010.